

# A New Sea Trial Method for Estimating Hydrodynamic Derivatives

Key-Pyo Rhee<sup>1</sup>, Kunho Kim<sup>2</sup>

<sup>1</sup>Dept. of Naval Architecture and Ocean Engineering, Seoul National University,  
Seoul, 151-742, KOREA

<sup>2</sup>Dept. of Naval Architecture and Marine Engineering, University of Michigan,  
Ann Arbor, MI 48105, U.S.A.

## Abstract

Estimation efficiencies according to different sea trials are investigated in connection with sensitivity analysis, and new trial method is proposed which can improve the estimation efficiency of hydrodynamic derivatives. MMG Equation with Kijima's formula is used for simulation. Extended Kalman Filter is chosen for estimation technique and hydrodynamic derivatives of interest is limited to 12 of those in sway and yaw equations. Esso Osaka is selected for the test ship. Sensitivity analysis and estimation results based on conventional trials show that a more sensitive derivative gives more efficient estimation result. Sensitivities of nonlinear derivatives become pronounced in the trial where steady condition lasts longer such as turning test, while sensitivities of linear derivatives has a larger values in the trial where unsteady condition lasts longer such as 10deg-10deg zigzag test. Consequently, in new method, named S-type trial, steady and unsteady condition are combined appropriately to increase sensitivities. Linear derivatives are estimated better in S-type trial and the estimation of nonlinear derivatives is improved to some extent.

## 1 Introduction

The manoeuvrability of a ship is predicted by several ways. One of them is a direct method by a free running test of model ship. Another is an indirect method using the hydrodynamic derivatives estimated by captive model tests. The latter one, however, has its limitation due to the scale effect. Therefore it is necessary to estimate the hydrodynamic derivatives by ship trials.

System identification for estimating the hydrodynamic derivatives of a ship dated from 1970's. Hwang[Hwang, 1980] estimated the hydrodynamic derivatives of Esso Osaka by Extended Kalman Filter using the data from turning and zigzag test. In doing this so called simultaneous drift, which is a phenomenon some derivatives are drifting to wrong values together, presented itself. Kang[Kang et al., 1984] suggested the input where the ratio of sway to yaw velocity is different as the remedy of simultaneous drift, and Ahn[Ahn, 1992] introduced the second order filter in the estimation of derivatives. Lee[Lee et al., 1995] researched the estimation by second order filter and parallel processing and showed that second order filter is not so different from Extended Kalman Filter. Besides, Hwang[Hwang, 1996] tried to change the equations of motion by the thought

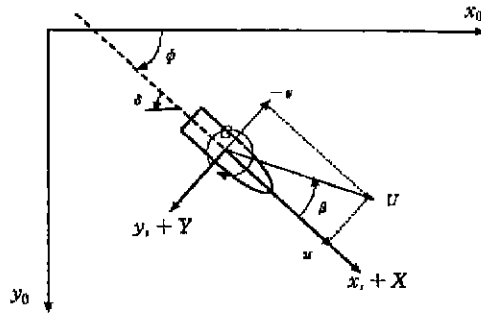


Figure 1. Coordinate system.

that the problem was resulted from higher order terms, which have no physical meaning, in the equations.

In this paper hydrodynamic coefficients are estimated using simulated data of turning and zigzag tests and the estimation performances are analyzed by coefficient sensitivity and a new trial scheme is suggested to raise the estimation efficiency.

## 2 Equation of Motion

### 2.1 Equation of motion

MMG equation[Hirano, 1980] divides the force into the force acting on hull, propeller, rudder and so on. Moreover it considers the interaction between hull, propeller and rudder. Therefore, it is known to describe the motion of ship better than other models. In case center of gravity is taken as the center of coordinate, the equation of motion is as follows,

$$(m - X_{\dot{u}})\dot{u} - (m - Y_v)vr = X_H + X_P + X_R, \quad (1)$$

$$(m - Y_{\dot{v}})\dot{v} + (m - X_{\dot{u}})ur = Y_H + Y_R, \quad (2)$$

$$(I_{zz} - N_{\dot{r}})\dot{r} = N_H + N_R. \quad (3)$$

where, subscript H corresponds to hull, P to propeller and R to rudder. Environmental forces due to wind, wave, and current are neglected and  $Y$  force due to propeller is neglected. In Equations (1)-(3), the forces on right hand side can be expressed by several ways. The equations of propeller and rudder force are settled in some extent by recent researches. but the expression of hull force has not been set up yet. So, various expressions are used now.

The coordinate used in this paper is shown in Figure 1 as same as MMG's.

The Kijima model[Japan Institute of Navigation, 1995] is used to express hull force. It is noted that drift angle  $\beta$  is used instead of sway velocity  $v$ . The equations are as follows,

**Table 1.** Principal particulars of Esso Osaka.

particulars	dimensions
$L(m)$	325.00
$B(m)$	53.00
$T(m)$	21.73
$C_b$	0.831
$A_w(m^2)$	27313.50
$D_P(m)$	9.10
$P(m)$	6.51
$A_R(m^2)$	119.82
$H_R(m)$	13.85
$L_R(m)$	9.00
$\delta_{max} (^\circ)$	35.00
$\dot{\delta}_{max} (^\circ/s)$	2.34

$$X_H = X_{\beta r} \left[ \frac{\rho}{2} L^2 T U \right] r \sin \beta + X_{uv} \left[ \frac{\rho}{2} L T U^2 \right] \cos^2 \beta, \quad (4)$$

$$Y_H = Y_0 \left[ \frac{\rho}{2} L T U^2 \right] + Y_\beta \left[ \frac{\rho}{2} L T U^2 \right] \beta + Y_r \left[ \frac{\rho}{2} L^2 T U \right] r + Y_{\beta|\beta|} \left[ \frac{\rho}{2} L T U^2 \right] \beta|\beta| \\ + Y_{r|r|} \left[ \frac{\rho}{2} L^3 T \right] r|r| + Y_{\beta\beta r} \left[ \frac{\rho}{2} L^2 T U \right] \beta\beta r + Y_{\beta r r} \left[ \frac{\rho}{2} L^3 T \right] \beta r r, \quad (5)$$

$$N_H = N_0 \left[ \frac{\rho}{2} L^2 T U^2 \right] + N_\beta \left[ \frac{\rho}{2} L^2 T U^2 \right] \beta + N_r \left[ \frac{\rho}{2} L^3 T U \right] r + N_{\beta|\beta|} \left[ \frac{\rho}{2} L^2 T U^2 \right] \beta|\beta| \\ + N_{r|r|} \left[ \frac{\rho}{2} L^4 T \right] r|r| + N_{\beta\beta r} \left[ \frac{\rho}{2} L^3 T U \right] \beta\beta r + N_{\beta r r} \left[ \frac{\rho}{2} L^4 T \right] \beta r r. \quad (6)$$

The compensation factor for longitudinal  $v - r$  coupled term,  $c_m$  is as follows,

$$c_m = \frac{X_{vr} - Y_{\dot{v}}}{-Y_{\dot{v}}}. \quad (7)$$

Noting that the signs of  $X_{vr}$  and  $X_{\beta r}$ ,  $X_{\beta r}$  expressed as follows.

$$X_{\beta r} = (c_m - 1) Y_{\dot{v}}. \quad (8)$$

Kijima suggested prediction formula for the hydrodynamic derivatives of  $Y$  and  $N$  by regression of experimental data. This formulae predict nonlinear derivatives as well as linear derivatives. The formulae for linear derivatives are same as those of Inoue et al. [Inoue et al., 1981] except  $Y_r$ . Kijima's prediction formula for a ship without trim are adopted for this research. The forces acting on propeller and rudder are estimated by use of empirical formula by MMG.

## 2.2 Simulation

Esso Osaka is taken as the model ship, which is the manoeuvrability standard ship of ITTC. The principal dimensions of Esso Osaka are shown in Table 1.

Simulation program is made to print out time, latitude, longitude, heading angle, ship speed and propeller rpm at every five seconds. This is same format as real ship trial data.  $u, v, r, \delta$  are also printed to be checked.

First,  $\dot{x}_G, \dot{y}_G$  are calculated using  $u, v, r$  and  $\psi$  as follows,

$$\begin{aligned} \dot{x}_G &= u \cos \psi - v \sin \psi, \\ \dot{y}_G &= u \sin \psi + v \cos \psi. \end{aligned} \quad (9)$$

Next, the changes of  $x_G$  and  $y_G$  are converted to the changes of latitude and longitude respectively. These changes are added to the start point.  $1^\circ$  in latitude is taken  $1852 \times 60$  (m) and longitude  $1^\circ$  as  $1526.16 \times 60$  (m).

In next section, the details of the computation of the forces will be presented.

### 2.2.1 Hull Force

The inertia coefficients of Esso Osaka are taken from [Japan Institute of Navigation, 1987].  $c_{rn}$  used in computation of  $X_{\beta r}$  is fitted by 1st order polynomial of  $C_b$  using the graph in [Japan Institute of Navigation, 1995] as follows,

$$c_{rn} = -0.484 + 1.643C_b. \quad (10)$$

$X_{uu}$  is computed by following equation using the total resistance coefficient  $C_r (= 0.002256)$  from Hwang[Hwang, 1980].

$$X_{uu} = -\frac{A_w}{L T} C_r. \quad (11)$$

The derivatives of  $Y$  and  $N$  are computed by Kijima's prediction formulae.  $Y_0$  and  $N_0$  are taken from Hwang[Hwang, 1980]. The derivatives of Esso Osaka are shown in Table 2. In this paper, the trial data are made from the simulation using the derivatives in Table 3, then the derivatives are estimated using these data. Therefore, it is noted that these values are considered as real value in estimation.

**Table 2.** Hydrodynamic derivatives of Esso Osaka.

coeff.	values	coeff.	values
$X_{\beta r}$	+0.278E-1	$X_{uu}$	-0.873E-2
$Y_0$	+0.2991E-3	$N_0$	-0.1496E-3
$Y_\beta$	+0.3998	$N_\beta$	+0.1337
$Y_r$	+0.8774E-1	$N_r$	-0.5433E-1
$Y_{\beta\beta}$	+0.6732	$N_{\beta\beta}$	-0.5180E-3
$Y_{rr}$	+0.4686E-1	$N_{rr}$	-0.2224E-1
$Y_{\beta\beta r}$	-0.1389	$N_{\beta\beta r}$	-0.1625
$Y_{\beta rr}$	+0.4123	$N_{\beta rr}$	-0.1204

**Table 1.** Principal particulars of Esso Osaka.

particulars	dimensions
$L(m)$	325.00
$B(m)$	53.00
$T(m)$	21.73
$C_b$	0.831
$A_w(m^2)$	27313.50
$D_P(m)$	9.10
$P(m)$	6.51
$A_R(m^2)$	119.82
$H_R(m)$	13.85
$L_R(m)$	9.00
$\delta_{max}(^\circ)$	35.00
$\dot{\delta}_{max}(^\circ/s)$	2.34

$$X_H = X_{\beta r} \left[ \frac{\rho}{2} L^2 T U \right] r \sin \beta + X_{uv} \left[ \frac{\rho}{2} L T U^2 \right] \cos^2 \beta, \quad (4)$$

$$Y_H = Y_0 \left[ \frac{\rho}{2} L T U^2 \right] + Y_\beta \left[ \frac{\rho}{2} L T U^2 \right] \beta + Y_r \left[ \frac{\rho}{2} L^2 T U \right] r + Y_{\beta|\beta|} \left[ \frac{\rho}{2} L T U^2 \right] \beta|\beta| \\ + Y_{r|r|} \left[ \frac{\rho}{2} L^3 T \right] r|r| + Y_{\beta\beta r} \left[ \frac{\rho}{2} L^2 T U \right] \beta\beta r + Y_{\beta r r} \left[ \frac{\rho}{2} L^3 T \right] \beta r r, \quad (5)$$

$$N_H = N_0 \left[ \frac{\rho}{2} L^2 T U^2 \right] + N_\beta \left[ \frac{\rho}{2} L^2 T U^2 \right] \beta + N_r \left[ \frac{\rho}{2} L^3 T U \right] r + N_{\beta|\beta|} \left[ \frac{\rho}{2} L^2 T U^2 \right] \beta|\beta| \\ + N_{r|r|} \left[ \frac{\rho}{2} L^4 T \right] r|r| + N_{\beta\beta r} \left[ \frac{\rho}{2} L^3 T U \right] \beta\beta r + N_{\beta r r} \left[ \frac{\rho}{2} L^4 T \right] \beta r r. \quad (6)$$

The compensation factor for longitudinal  $v - r$  coupled term.  $c_m$  is as follows,

$$c_m = \frac{X_{vr} - Y_{\dot{v}}}{-Y_{\dot{v}}}. \quad (7)$$

Noting that the signs of  $X_{vr}$  and  $X_{\beta r}$ ,  $X_{\beta r}$  expressed as follows.

$$X_{\beta r} = (c_m - 1)Y_{\dot{v}}. \quad (8)$$

Kijima suggested prediction formula for the hydrodynamic derivatives of  $Y$  and  $N$  by regression of experimental data. This formulae predict nonlinear derivatives as well as linear derivatives. The formulae for linear derivatives are same as those of Inoue et al.[Inoue et al., 1981] except  $Y_r$ . Kijima's prediction formula for a ship without trim are adopted for this research. The forces acting on propeller and rudder are estimated by use of empirical formula by MMG.

## 2.2 Simulation

Esso Osaka is taken as the model ship, which is the manoeuvrability standard ship of ITTC. The principal dimensions of Esso Osaka are shown in Table 1.

Simulation program is made to print out time, latitude, longitude, heading angle, ship speed and propeller rpm at every five seconds. This is same format as real ship trial data.  $u, v, r, \delta$  are also printed to be checked.

First,  $\dot{x}_G, \dot{y}_G$  are calculated using  $u, v, r$  and  $\psi$  as follows,

$$\begin{aligned} \dot{x}_G &= u \cos \psi - v \sin \psi, \\ \dot{y}_G &= u \sin \psi + v \cos \psi. \end{aligned} \quad (9)$$

Next, the changes of  $x_G$  and  $y_G$  are converted to the changes of latitude and longitude respectively. These changes are added to the start point.  $1^\circ$  in latitude is taken  $1852 \times 60$  (m) and longitude  $1^\circ$  as  $1526.16 \times 60$  (m).

In next section, the details of the computation of the forces will be presented.

### 2.2.1 Hull Force

The inertia coefficients of Esso Osaka are taken from [Japan Institute of Navigation, 1987].  $c_m$  used in computation of  $X_{\beta r}$  is fitted by 1st order polynomial of  $C_b$  using the graph in [Japan Institute of Navigation, 1995] as follows,

$$c_m = -0.484 + 1.643C_b. \quad (10)$$

$X_{uu}$  is computed by following equation using the total resistance coefficient  $C_r (= 0.002256)$  from Hwang[Hwang, 1980].

$$X_{uu} = -\frac{A_w}{L T} C_r. \quad (11)$$

The derivatives of  $Y$  and  $N$  are computed by Kijima's prediction formulac.  $Y_0$  and  $N_0$  are taken from Hwang[Hwang, 1980]. The derivatives of Esso Osaka are shown in Table 2. In this paper, the trial data are made from the simulation using the derivatives in Table 3, then the derivatives are estimated using these data. Therefore, it is noted that these values are considered as real value in estimation.

**Table 2.** Hydrodynamic derivatives of Esso Osaka.

coeff.	values	coeff.	values
$X_{\beta r}$	+0.278E-1	$X_{uu}$	-0.873E-2
$Y_0$	+0.2991E-3	$N_0$	-0.1496E-3
$Y_\beta$	+0.3998	$N_\beta$	+0.1337
$Y_r$	+0.8774E-1	$N_r$	-0.5433E-1
$Y_{\beta\beta}$	+0.6732	$N_{\beta\beta}$	-0.5180E-3
$Y_{rr}$	+0.4686E-1	$N_{rr}$	-0.2224E-1
$Y_{\beta\beta r}$	-0.1389	$N_{\beta\beta r}$	-0.1625
$Y_{\beta r r}$	+0.4123	$N_{\beta r r}$	-0.1204

**Table 3.** Values for calculating rudder force.

coeff.	value
$\eta$	0.657
$\lambda$	1.539
$C_N$	2.490
$\gamma$	0.275
$\epsilon$	1.009
$t_R$	0.217
$a_H$	0.865
$x_H$	-0.181

### 2.2.2 Propeller Force

Thrust coefficient  $K_T$ , thrust deduction factor  $t_{p0}$ , effective wake fraction on propeller  $w_{p0}$  are computed by the fitted functions using the open water test data [KIMM, 1988]. These functions are as follows,

$$K_T = 0.3493 - 0.3340J_P - 0.1509J_P^2 + 0.0102J_P^3, \quad (12)$$

$$t_{p0} = 0.1093 + 0.0296u - 0.0032u^2 + 0.000115u^3, \quad (13)$$

$$w_{p0} = 0.2616 + 0.0253u - 0.0034u^2 + 0.00013u^3. \quad (14)$$

Propeller rps,  $n$  is computed as following equation[Son, 1989].

$$2\pi(I_{Pp} + J_{Pp})\dot{n} = Q_P + Q_E \quad (15)$$

where,  $I_{Pp}$  is the polar mass moment of inertia of propeller and its shaft, and  $J_{Pp}$  is the polar added mass moment of inertia of them. These are approximated as follows,

$$(I_{Pp} + J_{Pp}) = 2.0 D_P^5 \quad (16)$$

Propeller torque  $Q_P$  is expressed as follows.

$$Q_P = -\rho n^2 D_P^5 K_Q(J_P) \quad (17)$$

The torque of main engine,  $Q_E$  is as follows in the case of steam turbine which keeps the power constant during trial.

$$Q_E = \frac{745 \text{ SHP}_0}{2\pi n} \quad (18)$$

where,  $\text{SHP}_0$  is the effective shaft horse power of main engine in straight forward condition in the PS dimension. It is computed by the fitted function of  $u$  using experimental data[Inoue et al., 1988]. The fitted function is as follows,

**Table 4.** Other conditions.

$n_0$ (initial rpm)	54.12
$t_f$ (final time, sec)	3000
$t_{step}$ (time step, sec)	5.0
Noise Level of Latitude ( $^{\circ}$ )	8.0E-7
Noise Level of Longitude ( $^{\circ}$ )	4.0E-7
Noise Level of $\psi$ ( $^{\circ}$ )	1.2E-2
Noise Level of n (rpm)	2.0E-1

**Table 5.** Difference sums in trial 1.

coeff.	diff. of $u$	diff. of $v$	diff. of $r$
...	...	...	...
$c_1$	$u_{11}$	$v_{11}$	$r_{11}$
...	...	...	...
Sum	$s_{u1}$	$s_{v1}$	$s_{r1}$

**Table 6.** Difference sums in trial 2.

coeff.	diff. of $u$	diff. of $v$	diff. of $r$
...	...	...	...
$c_1$	$u_{12}$	$v_{12}$	$r_{12}$
...	...	...	...
Sum	$s_{u2}$	$s_{v2}$	$s_{r2}$

$$SHP_0 = -601.1 + 632.0 u - 182.0 u^2 + 74.7 u^3. \quad (19)$$

### 2.2.3 Rudder Force

Rudder force can be computed by the equations in section 2.2.2 which follows [Japan Institute of Navigation, 1995]. The values in need are shown in Table 4.

The mathematical model of steering gear is that of electromotive oil pressure gear as shown below [Son, 1989].

$$\dot{\delta} = \begin{cases} (\delta^* - \delta)/T_E & ; |\delta^* - \delta| \leq T_E |\dot{\delta}_{max}| \\ \text{sign}(\delta^* - \delta) |\dot{\delta}_{max}| & ; |\delta^* - \delta| > T_E |\dot{\delta}_{max}| \end{cases} \quad (20)$$

where,  $\delta^*$  is ordered rudder angle and  $T_E$  is the time constant,  $|\dot{\delta}_{max}|$  is the maximum rudder angular velocity in rad/sec. In this paper  $T_E$  is 2.5 (sec).

### 2.2.4 Other Conditions

The initial velocity is set to 10 knots for all trials, thus there exists only surge velocity in initial stage. The initial rpm,  $n_0$ , for this speed can be found by equating the surge equation. That is, the initial steady rpm is the rpm which makes the right side of surge equation equal to zero. Simulation time  $t_f$  is determined to make the ship turns 560 deg. Time condition is summarized in Table 5. Measurement noise is generated by adding random values to simulation data. These random values are those between predetermined levels. For example, if the noise level of latitude is 8.0E-7, then the random values between +8.0E-7 and -8.0E-7 are added to the latitude. These conditions are summarized in Table 5.



**Table 7.** Initial state values and initial error covariance.

state	initial value	initial covariance	state	initial value	initial covariance
$u$	10.0 (knots)	0.5 (m/s)	$Y_{\beta\beta r}$	-0.1667	0.07
$v$	0.0	0.1 (m/s)	$Y_{\beta rr}$	+0.4947	0.2
$r$	0.0	0.1 (/s)	$N_{\beta}$	+0.1605	0.07
$n$	54.21 (rpm)	0.1 (rps)	$N_r$	-0.6519E-1	0.03
$Y_{\beta}$	+0.480	0.2	$N_{\beta\beta}$	-0.6216E-3	0.0002
$Y_r$	+0.1053	0.04	$N_{rr}$	-0.2669E-1	0.01
$Y_{\beta\beta}$	+0.8079	0.3	$N_{\beta\beta r}$	-0.1950	0.08
$Y_{rr}$	+0.5624E-1	0.02	$N_{\beta rr}$	-0.1444	0.06

**Table 8.** Measurement error covariance.

	ST35	ZZ10	ZZ20
$R_{11}(u)$	5.0E-2	1.0E-1	8.0E-2
$R_{22}(v)$	7.0E-2	4.0E-2	6.0E-2
$R_{33}(r)$	3.0E-4	2.0E-4	2.0E-4
$R_{44}(n)$	5.0E-1	4.0E-1	4.0E-1

**Table 9.** Estimation Errors (%)

coeff.	ST35	ZZ10	ZZ20
$Y_{\beta}$	2.65	2.26	0.85
$Y_r$	5.04	3.03	1.37
$Y_{\beta\beta}$	6.86	9.73	3.23
$Y_{rr}$	16.74	14.98	9.54
$Y_{\beta\beta r}$	29.07	22.84	27.64
$Y_{\beta rr}$	3.96	14.38	6.94
$N_{\beta}$	1.91	0.82	0.01
$N_r$	2.21	0.48	0.97
$N_{\beta\beta}$	15.32	14.95	1.19
$N_{rr}$	3.75	31.05	14.42
$N_{\beta\beta r}$	8.73	18.32	10.27
$N_{\beta rr}$	2.89	15.81	3.72

### 3 Sensitivity Analysis

#### 3.1 Sensitivity

The system identification method is applied to estimate the hydrodynamic derivatives in ship manoeuvring equations. If some coefficients can be determined uniquely by the relation of input and output, those coefficients can be thought identifiable. This identifiability can be related to the contribution of coefficient to the system. That is, if there is no effect of a coefficient on the system, it is almost impossible to estimate the coefficient from input and output data. On the other hand, if the coefficient have significant effect on the system, it becomes more identifiable.

For this reason, it is very important to check these identifiabilities before estimating derivatives. To examine the identifiability of a derivative, it is necessary to express the effect of each derivative on the system by some numerical value. This value is called the sensitivity of the derivative.

### 3.2 Sensitivity Analysis

There are several ways to define sensitivity. In this paper, Hwang's method is modified[Hwang, 1980]. Since estimation is carried out by velocities, the change of velocities to the change of a derivative is defined as the sensitivity of the derivative.

Hwang's method is good to compare the sensitivities in one trial, and relative effect in different trials. However, his method is not appropriate to compare the sensitivity of a certain derivative in various trials. Moreover since it uses the maximum difference, if the difference becomes abnormally large at certain time, the sensitivity of that derivative might be computed by that abnormal difference.

Therefore the method is modified to compare the sensitivity of a derivative directly. The modified method uses the sums of differences during trial instead of maximum differences in order to avoid unexpected large sensitivity due to irregular single maximum differences.

For example, the computation of the sensitivities of derivatives in trial 1 and trial 2 follows these steps.

- 1) Simulate trial 1 with unperturbed derivatives. Save it.
- 2) Perturb a particular derivative, say  $c_i$ , into 120% of its value and simulate trial 1 again.
- 3) Return  $c_i$  to unperturbed value.
- 4) Repeat (2)-(3) for each derivative and save the result.
- 5) Add all the differences between unperturbed(1) and perturbed(2) data.
- 6) Repeat (1)-(4) for trial 2.

In this way, we can make Table 8 and Table 9, then the sensitivity of  $c_1$  in trial 1 is as follows,

$$S'_{c_1,1} = \frac{u_{11}}{s_{u1} + s_{u2}} + \frac{v_{11}}{s_{v1} + s_{v2}} + \frac{r_{11}}{s_{r1} + s_{r2}}. \quad (21)$$

The sensitivity is defined as percentile value of  $S'_{c_1,1}$ . In other words, the sums of  $S_{c_i,1}$ s in trial 1 or trial 2 comes to three, therefore each sensitivity value is divided by three and multiplied by 100, as follows,

$$S_{c_1,1} = \frac{S'_{c_1,1}}{3} \times 100. \quad (22)$$

Note that the sensitivity of a derivative is different according to the kinds of trials being compared.

The sensitivities in conventional trials are shown in Figure 2. In the figure, 35deg starboard turning test is denoted by ST35, 10deg-10deg zigzag test by ZZ10 and 20deg-20deg zigzag test by ZZ20. Subscript 'b' represents  $\beta$ . From the results, it is found that the sensitivities of linear derivatives are larger in zigzag test than turning test and in zigzag tests these sensitivities are larger in 10deg-10deg than those in 20deg-20deg, while the sensitivities of nonlinear derivatives are larger in turning than in zigzag and larger in 20-20 zigzag than in 10deg-10deg zigzag. This phenomenon can be explained by the fact that the contribution of linear derivatives becomes greater as manoeuvre becomes gentler while that of nonlinear derivatives becomes greater as manoeuvre gets steeper. In other words, the contribution of nonlinear derivatives becomes greater as

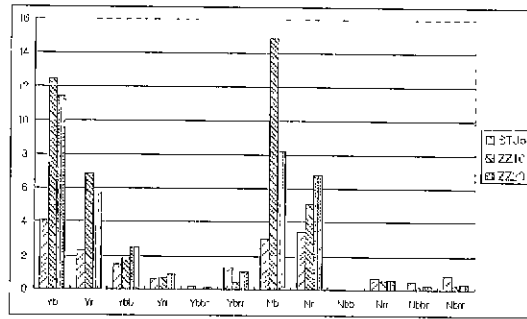


Figure 2. Sensitivity analysis in conventional trials.

steady state lasts longer while that of linear derivatives becomes larger as unsteady state appears more frequently. Therefore, since the steady state in 20deg-20deg zigzag test is longer than that of 10deg-10deg zigzag, the sensitivities of nonlinear derivatives become large.

As shown in Figure 2, the sensitivities of nonlinear derivatives are relatively small compared with linear ones, which means their contribution to the system are very small. Especially the sensitivities of  $Y_{\beta\beta r}$  and  $N_{\beta\beta}$  are very small among them. This can be explained by the fact that not only the values of the derivatives but also the terms including the derivatives are so small that the changes do not affect the system.

As sensitivity represents the contribution of a derivative, it can be expected that the derivative whose sensitivity is large will be estimated better. In next section, the estimation of derivatives will be presented to verify this assumption for conventional trials - ST35, ZZ10, ZZ20 - and this result will be compared with the result of sensitivity analysis in section 5.

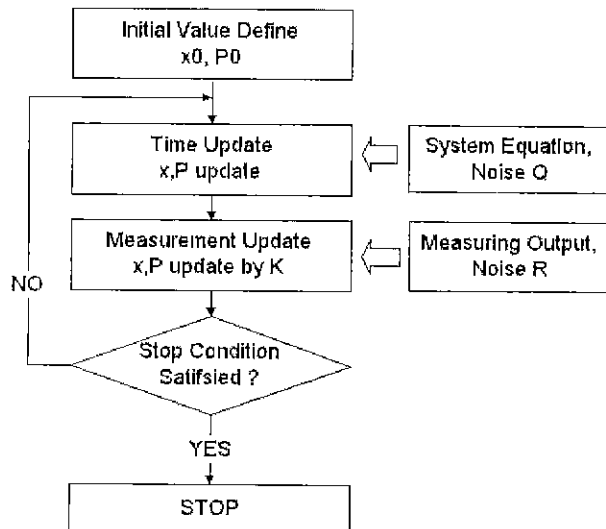


Figure 3. Estimation procedure.

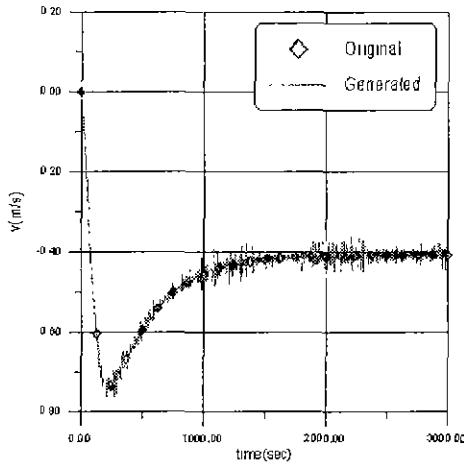


Figure 4. Generated  $v$  in ST35.

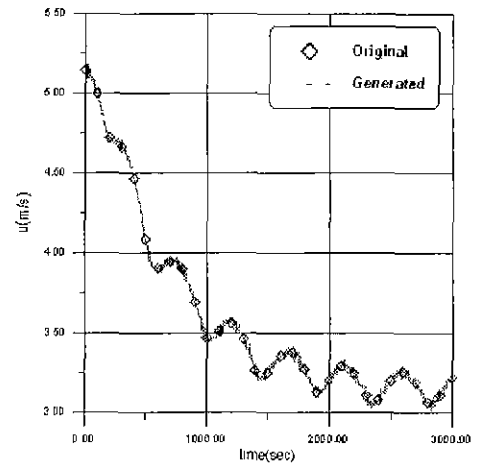


Figure 5. Generated  $u$  in ZZ20.

## 4 Estimation of Hydrodynamic Derivatives

### 4.1 Extended Kalman Filter

Kalman Filter is an optimal estimator in linear system whose states are stochastic and whose noises are white gaussian under the assumption that the estimated states and measurement are linear. In parameter estimation, however, since the equation of system is nonlinear, it is impossible to apply Kalman Filter, which is used in linear system, to nonlinear system. Consequently, Kalman Filter is modified into Extended Kalman Filter[Lewis, 1986] in order to be applied to nonlinear system.

Extended Kalman Filter estimates the states in real time by recursive time update and measurement update of the states and error covariance as time goes. Extended Kalman Filter estimates derivatives as well as states by including the derivatives as the states. These are called the augmented states. Therefore this filter is called as State Augmented Extended Kalman Filter(SAEKF). The estimation processes are outlined in Figure 3.

### 4.2 Estimation Method

In this sub-section the detailed estimation procedure is presented.

First, compute the values of 12 hydrodynamic derivatives using Kijima's formulae (9)-(10), and then simulate trials and save the data. These data consist of latitude, longitude, heading, and rpm but the data in need in estimation are velocities and rudder angle. Therefore, the information of heading angle, velocities and rudder angle are computed as following steps.

1. Interpolate the data of latitude, longitude etc. whose interval is 5.0 sec. into those of 0.1 sec. by interpolation. This interpolation is carried out by second order polynomial function fitted by three points.
2. Using the data of 0.1 sec. interval, compute  $x_G', y_G'$  and then compute  $u, v$ .
3.  $r$  is calculated by differentiating  $\psi$  numerically.

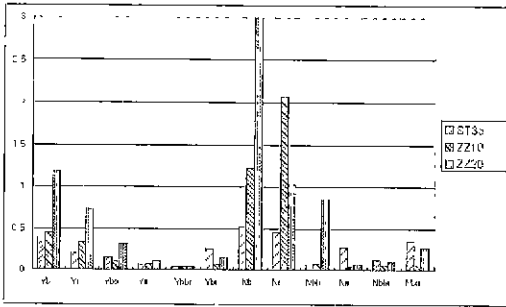


**Figure 6.** Estimation efficiency in conventional trials.

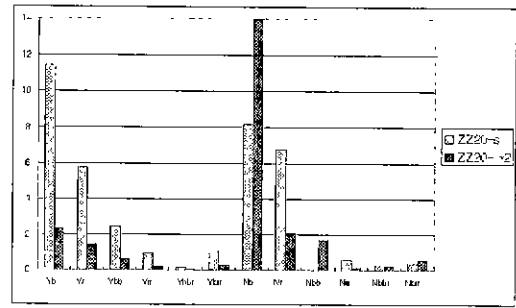


**Figure 7.** Relation between sensitivity and estimation fitness.

4.  $\delta$  is computed from heading angle change according to the kind of trial.

After computing  $u, v, r$  and  $\delta$  from raw data of latitude, longitude etc., these data will be compared to the original  $u, v, r$  and  $\delta$  printed by simulation program for confirmation. As shown in Figure 4 and Figure 5., the original data are well recovered with little noise.

In the estimation by Extended Kalman Filter, the choice of initial values of states and error covariance have considerable effect on estimation. In this paper the initial values of  $u, v, r$  and  $n$  are the real values, and the initial values of the derivatives are perturbed into 120 % of the real values. In the case using real trial data, the values from captive model tests can be used for initial values, or the values from prediction formulae. The initial values of error covariance are chosen by the values which have the same order of each state. The initial values of states and error covariance are summarized in Table 9.

The information of noise also has considerable influence on estimation. Since the simulation data are used in this study, system noise covariance  $Q$  is set to zero. In processing real data, it is expected that  $Q$  can be determined by analyzing real data and trial data. Measurement noise covariance  $R$  is determined by analyzing simulation data. From the results it is found that the case in which  $R$  is the double of the amplitude of noise gives the best results. Therefore,  $R$  is determined by analyzing  $u, v, r, n$  data. In real problem  $Q$  and  $R$  should be determined by engineering sense.

## 5 Estimation Using the Data of Conventional Trials

Hydrodynamic derivatives are estimated using the data from simulated starboard turning test, 10deg-10deg zigzag test and 20deg-20deg zigzag test. State variables are made up of surge velocity  $u$ , sway velocity  $v$ , yaw velocity  $r$ , propeller rps  $n$  and 12 augmented derivatives, so total number of states is 16.

Measurement error covariance  $R$  has only diagonal terms and these values are shown in Table 8.

The estimation efficiency is defined as the reciprocal of the final error. Estimation efficiencies of three trials are shown in Figure 6. The estimation efficiency of  $N_\beta$  in ZZ20 is over 100, thus considering other values in graph, y axis is limited to three. The percentile estimation errors are

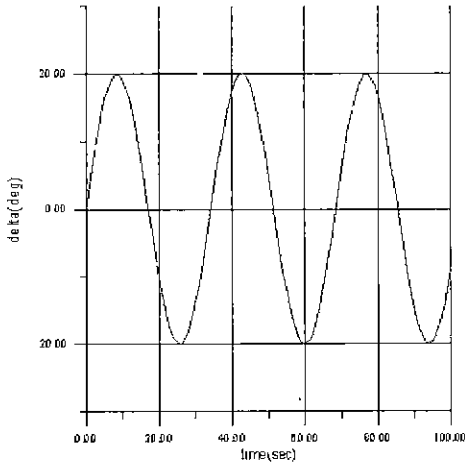


**Figure 8.** Sine manoeuvre.

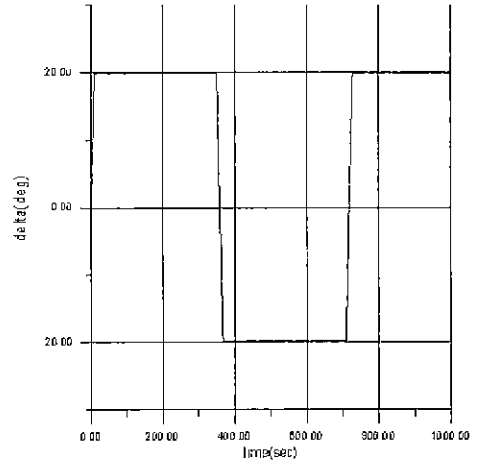


**Figure 9.** Sawteeth manoeuvre.

shown in Table 9.

From the estimation results, it is found that the linear derivatives are well estimated, while the estimation efficiency of nonlinear coefficients are not so high. The linear derivatives of  $Y$  and  $N$  are better estimated in zigzag test than in turning. This fact is in accordance with the expectation from the sensitivity analysis in section 4, that is, the estimation efficiencies of linear derivatives are higher in the trial in which unsteady conditions are more dominant than in the trial where steady conditions last longer. However, in zigzag test, the results from 20deg-20deg zigzag test are better than those from 10deg-10deg zigzag test except  $N_r$ . Although the efficiency of nonlinear derivatives are not so high, it can be found the efficiency in turning test is higher than that of zigzag tests. Besides, the estimation efficiency in 10deg-10deg zigzag test is higher than in 20deg-20deg zigzag test.

Next, the estimation results are analyzed with the sensitivity analysis. Figure 7 shows the sensitivities of derivatives and the estimation efficiency (fitness) in 20-20 zigzag test. 's' denotes sensitivity and 'e' means efficiency. It is found that the derivatives with higher sensitivities are better estimated than those of lower sensitivities. From this result it is expected that the nonlinear derivatives will be estimated better by using the data of the trial where the sensitivities of nonlinear derivatives are higher. In next section, a new trial method will be introduced based on these results.

## 6 New trial

From the results of previous section, it is found that the linear derivatives are well estimated but the nonlinear derivatives are not. Therefore, a couple of new trials are researched to improve the sensitivities of nonlinear derivatives. For this purpose, a trial method is needed which can improve the contribution of nonlinear derivatives.

In the first simulated trial, rudder is handled in sinusoidal fashion as shown in Figure 8. However, unlike the expectation, sensitivity analysis results show no improvement in the sensitivity of nonlinear derivatives.

In the second trial, rudder is operated steeply like Figure 9. This method seems to be similar to

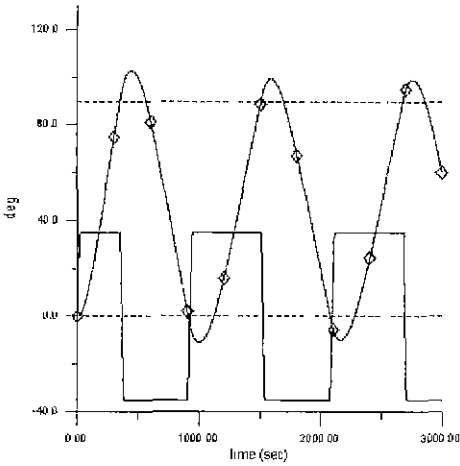


Figure 10. 90 deg S-type trials.

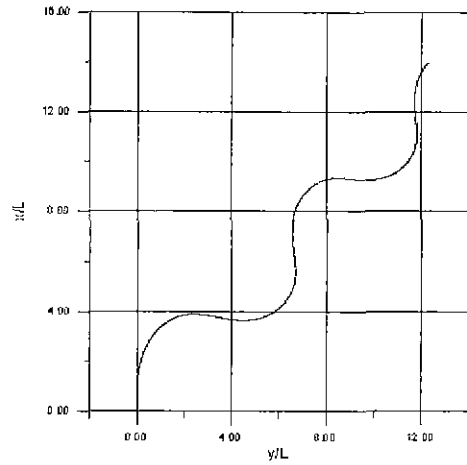


Figure 11. Trajectory of 90 deg S-type trial.

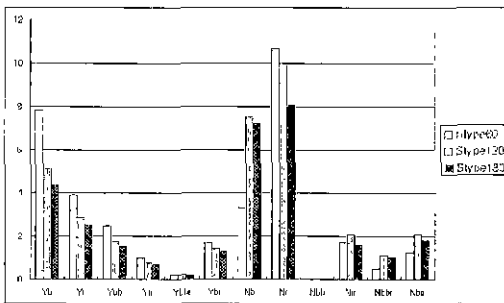


Figure 12. Sensitivity analysis between S-type trials.

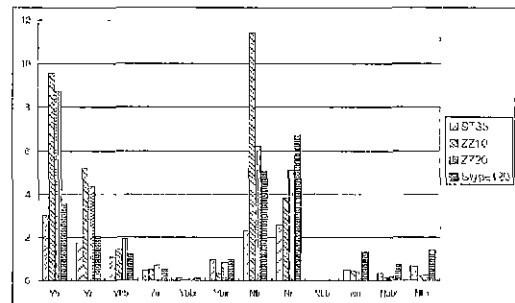


Figure 13. Comparison of sensitivity analysis b/w conventional trials and 120deg S-type trial.

zigzag test, but it is different in the sense that it does not consider the heading angle while zigzag test does. This is intended to improve the sensitivities of nonlinear derivatives by lasting the steady states longer and handling the rudder steeply which makes the system more excited. In spite of these efforts, this method also did not give satisfactory improvement of sensitivity.

From the results of above two cases and the sensitivity analysis of conventional trials, a trial in which steady and unsteady states are combined appropriately will be expected to improve the sensitivity of nonlinear derivatives. This improvement of sensitivities of nonlinear derivatives might decrease the estimation efficiencies of linear derivatives. However the overall estimation efficiency will be expected to be higher. This is because the sensitivities of linear derivatives are much higher than nonlinear derivatives.

### 6.1 S-Type Trial

As mentioned above, the sensitivity analyses in 35deg turning test and zigzag test show that the sensitivities of linear derivatives are comparatively large but those of nonlinear derivatives are so

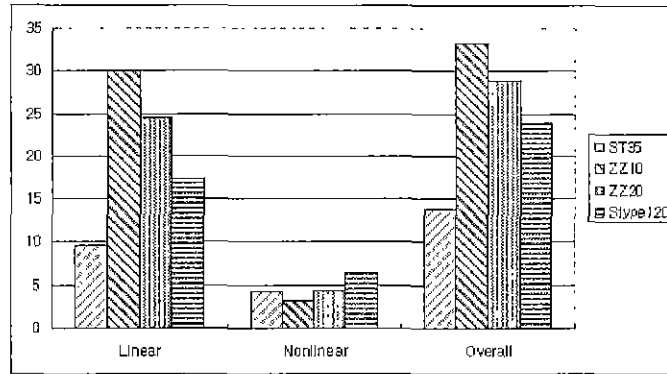


**Figure 14.** Sum of sensitivities in various trials.

small that it is almost impossible to estimate all the derivatives at once. Therefore a new trial method is required. The sensitivities of nonlinear derivatives in turning are larger than in zigzag test. However, this sensitivity values are not satisfactory.

From this result new trial method is designed. In this new method, turning test and zigzag test are combined. As mentioned in section 3, steady state lasts long in turning test and unsteady states occur repeatedly in zigzag test. This is the main reason why turning and zigzag are combined.

New trial method is named as S-type trial after the trajectory it makes. Figure 10 shows that the rudder angle and the heading angle in 90deg S-type trial. In case of  $\psi_S$ deg S-type trial, the ship goes like turning test until the heading becomes  $\psi_S$ deg and then the rudder angle is reversed to maximum. Then it goes on until the heading becomes zero and then the rudder is reversed to make the heading  $\psi_S$ deg again. This procedures are repeated like zigzag test. Figure 11 shows the trajectory made by 90deg S-type trial.

Before comparing S-type trials with conventional trials, three kinds of S-type trials - 60deg, 120deg, 180deg - are compared in sensitivity to determine which S-type trial is the best. Figure 12 shows the result that the sensitivities of  $Y$  derivatives decrease as the angle increases, and those of  $N$  derivatives are higher in 120deg than others. Considering these results and the trial condition, 120deg S-type trial is thought to be the best among them.

Next, 120deg S-type trial is compared with the conventional trials in the sensitivities of derivatives. As shown in Figure 13 the sensitivities of linear  $Y$  derivatives and  $N_\beta$  in 120deg S-type trial are smaller than in zigzag test and they are as good as turning test. The sensitivities of nonlinear  $Y$  derivatives are same as those of conventional trials or a little bit smaller but those of nonlinear derivatives of  $N$  in S-type trials are larger. To compare the sensitivities of S-type trial and conventional trials, the sums of linear, the sums of nonlinear and the total sums of sensitivities are shown in Figure 14. This figure shows that the total sum of sensitivities of S-type trial is lower than those of zigzag tests, but the sum of sensitivities of nonlinear derivatives is higher than others. This means that the sensitivities of nonlinear derivatives have increased as much. The sensitivities of linear derivatives are smaller than those of conventional trials but it is expected that the linear derivatives are not much affected by that in estimation.

Consequently it is found that the sensitivities of nonlinear derivatives increase in S-type trial. Next sub-section will show the estimation results from this S-type trial.



**Table 10.** Estimation result.

		ST35		ZZ10	
coeff.	real	final	err.(%)	final	err.(%)
$Y_{\beta}$	+0.3998	+0.3892	2.65	+0.3907	2.26
$Y_r$	+0.8774E-1	+0.9217E-1	5.04	+0.9041E-1	3.04
$Y_{\beta\beta}$	+0.6732	+0.7193	6.84	+0.7388	9.74
$Y_{rr}$	+0.4683E-1	+0.3902E-1	16.74	+0.3984E-1	14.98
$Y_{\beta\beta r}$	-0.1389	-0.1793	29.07	-0.1707	22.84
$Y_{\beta rr}$	+0.4123	+0.4286	3.96	+0.4716	14.38
$N_{\beta}$	+0.1337	+0.1363	1.91	+0.1326	0.82
$N_r$	-0.5433E-1	-0.5553E-1	2.21	-0.5459E-1	0.48
$N_{\beta\beta}$	-0.5180E-3	-0.5970E-3	15.33	-0.5950E-3	14.95
$N_{rr}$	-0.2224E-1	-0.2141E-1	3.76	-0.1534E-1	31.05
$N_{\beta\beta r}$	-0.1623	-0.1766	8.73	-0.1922	18.32
$N_{\beta rr}$	-0.1204	-0.1169	2.90	-0.1394	15.82
		ZZ20		S-Type120	
coeff.	real	final	err.(%)	final	err.(%)
$Y_{\beta}$	+0.3998	+0.3964	0.85	+0.3990	0.18
$Y_r$	+0.8774E-1	+0.8895E-1	1.37	+0.8859E-1	0.96
$Y_{\beta\beta}$	+0.6732	+0.6950	3.23	+0.6825	1.38
$Y_{rr}$	+0.4683E-1	+0.4240E-1	9.54	+0.4317E-1	7.88
$Y_{\beta\beta r}$	-0.1389	-0.1773	27.64	-0.1822	31.14
$Y_{\beta rr}$	+0.4123	+0.4409	6.94	+0.4350	5.50
$N_{\beta}$	+0.1337	+0.1337	0.01	+0.1350	0.90
$N_r$	-0.5433E-1	-0.5486E-1	0.97	-0.5524E-1	1.67
$N_{\beta\beta}$	-0.5180E-3	-0.5240E-3	1.19	-0.5540E-3	7.02
$N_{rr}$	-0.2224E-1	-0.1903E-1	14.42	-0.2070E-1	6.92
$N_{\beta\beta r}$	-0.1623	-0.1793	10.27	-0.1724	6.11
$N_{\beta rr}$	-0.1204	-0.1248	3.72	-0.1197	0.57

## 6.2 Estimation Using S-Type Trial Data

The estimation of derivatives is carried out using the data from 120deg S-type trial which is turned out to be the best S-type trial in the sense of sensitivities of derivatives. The conditions in estimation are exactly same as in the case of conventional trials. Figure 15 - Figure 26 show the result of estimation with those of conventional trials.

Figure 15 - Figure 18 show the estimation result of linear derivatives. As shown in the figures the estimation of linear derivatives are slightly improved in  $Y_{\beta}$  and  $Y_r$  but not in all cases. Figure 19 - Figure 22 show the estimation results of nonlinear  $Y$  derivatives. The result of  $Y_{\beta\beta r}$  is very poor and there should be more study about this. Other derivatives of  $Y$  are generally better estimated in S-type trial. Figure 23 - Figure 26 show the estimation results of nonlinear derivatives of  $N$ . The convergence and estimation efficiencies of  $N_{\beta\beta}$  and  $N_{\beta\beta r}$  are not satisfactory. The value of  $N_{\beta\beta}$  is so small that it is thought to be very sensitive to the noise. The estimation efficiencies of  $N_{\beta\beta r}$  and  $N_{\beta rr}$  in S-type trial are higher than others as same as the case of nonlinear derivatives of  $Y$ . The estimation results are summarized in Table 10.

In this time the estimation efficiencies are compared by the trajectory of 20deg-20deg zigzag

test, In Figure 27, the trajectory by the derivatives estimated from S-type trial is denoted by star. In general all trajectories are almost same as the real trajectories, so it is hard to know the difference. However, close inspection shows that the trajectories using the S-type test results are closer to the real one than others. The trajectories using the derivatives estimated from 20deg-20deg zigzag and S-type are almost same as the real one.

Next, the sums of estimation efficiencies in linear, nonlinear and overall are inspected. Figure 28 shows the efficiencies divided into three categories of linear, nonlinear, and overall. For example, the efficiency of linear derivatives is computed by adding all the estimation errors of linear derivatives and taking the reciprocal value of it. The normalized values of these efficiencies are shown in the figure. As shown in the figure, the linear derivatives are best estimated in 20deg-20deg zigzag and the second best in S-type. Nonlinear derivatives are best estimated in S-type trial as expected. The overall estimation efficiency in S-type trial is higher than others. This advance is believed to result from the improvement of the estimation efficiency of nonlinear derivatives.

## 7 Conclusions

In this paper a procedure to estimate the hydrodynamic derivatives using simulated sea trial data is studied and a new trial method, so called, S-type trial is suggested to improve the estimation efficiencies.

From the sensitivity analysis of derivatives, it is found that the sensitivities of nonlinear derivatives in 35deg turning test where steady state is long are greater than others and the sensitivities of linear derivatives are large in zigzag test in which unsteady state continuously repeated.

The estimation results from conventional trials show that the linear derivatives are much better estimated than the nonlinear derivatives and that generally linear derivatives are estimated better in zigzag than turning and nonlinear derivatives are better in turning than zigzag tests.

The sensitivities of linear derivatives in S-type trial are smaller than conventional trials but those of nonlinear derivatives become larger. The estimation result shows that the estimation of linear derivatives from S-type trial is not good as that of 20deg-20deg zigzag, however, it is better than turning and 10deg-10deg zigzag. The nonlinear derivatives are estimated better in S-type trials than others. Following is the summary of the results mentioned above.

First, the estimation efficiency of a derivative is related to its sensitivity and the derivative with higher sensitivity is generally estimated better.

Second, nonlinear derivatives have larger contribution to the system in the trial where steady state lasts longer such as turning test than other tests. Consequently, the estimation of nonlinear derivatives is more efficient in such test rather than other tests. On the other hand, linear derivatives show larger contribution in the trial where unsteady state appears repeatedly such as zigzag test and accordingly the estimation of linear ones become more efficient.

Third, the results using S-type trial show that the estimation efficiencies of nonlinear derivatives are improved and those of linear ones are still good. The overall estimation efficiency in S-type trial is higher than others.

## Acknowledgements

This work was sponsored by the Research Institute of Marine Systems Engineering, College of Engineering, Seoul National University.

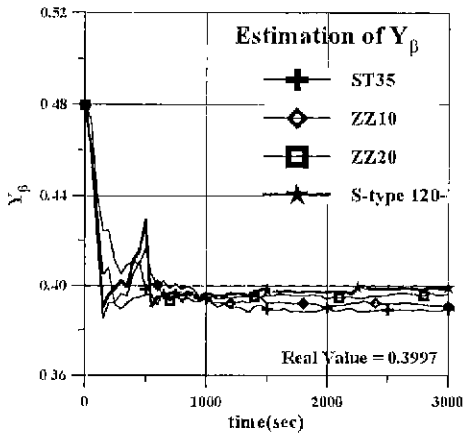


Figure 15. Estimation of  $Y_{\beta}$ .

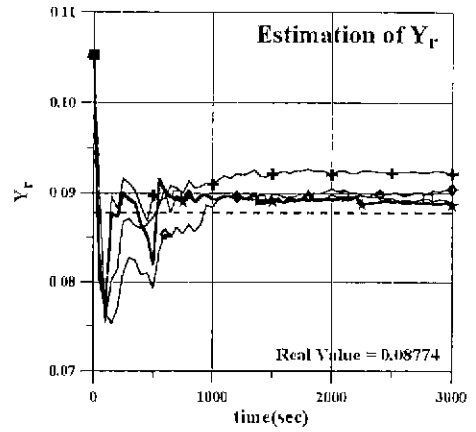


Figure 16. Estimation of  $Y_r$ .

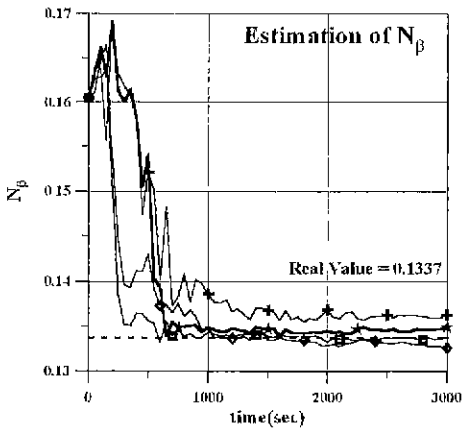


Figure 17. Estimation of  $N_{\beta}$ .

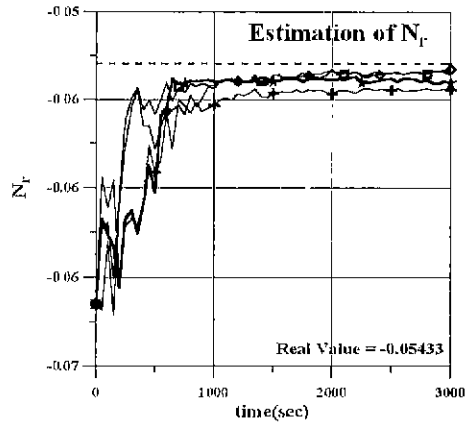


Figure 18. Estimation of  $N_r$ .

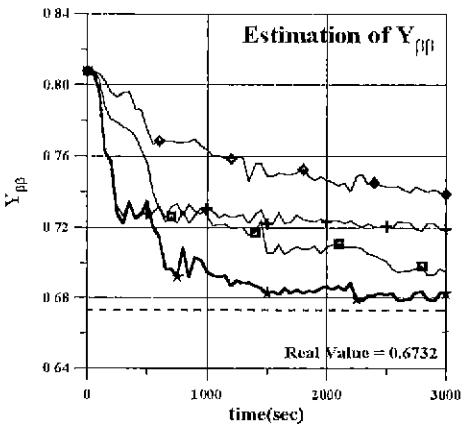


Figure 19. Estimation of  $Y_{\beta\beta}$ .

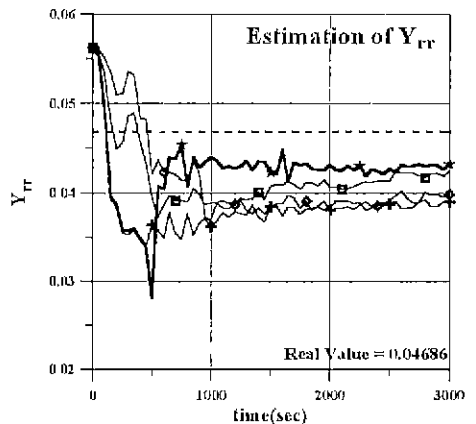


Figure 20. Estimation of  $Y_{rr}$ .

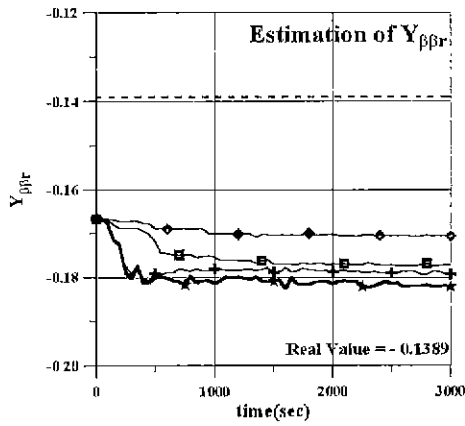


Figure 21. Estimation of  $Y_{\beta\beta r}$ .

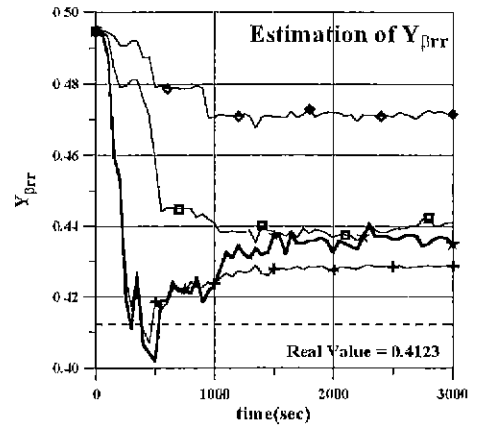


Figure 22. Estimation of  $Y_{\beta r r}$ .

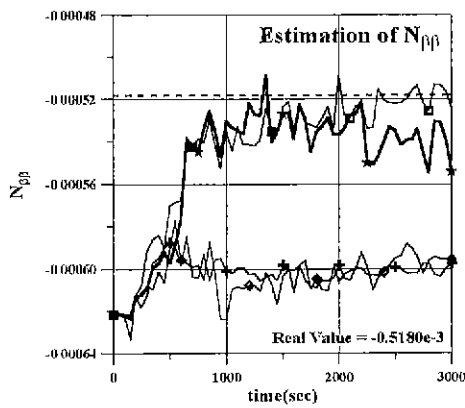


Figure 23. Estimation of  $N_{\beta\beta}$ .

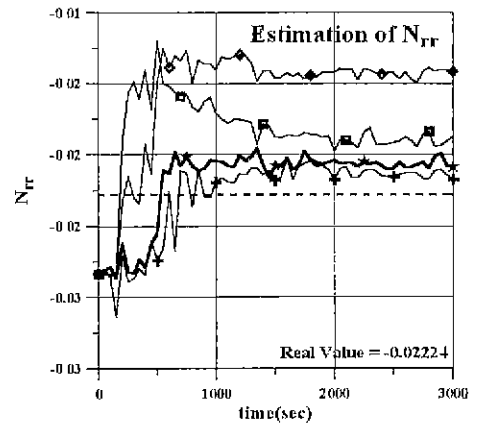


Figure 24. Estimation of  $N_{r r}$ .

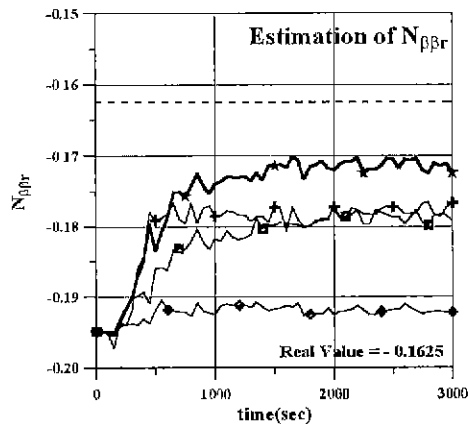


Figure 25. Estimation of  $N_{\beta\beta r}$ .

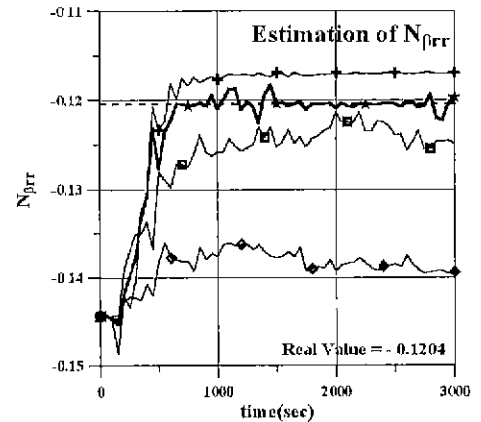


Figure 26. Estimation of  $N_{\beta r r}$ .

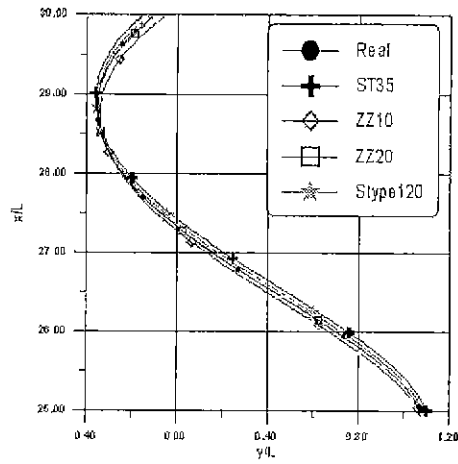


Figure 27. Trajectory of 20deg-20deg zigzag trials with estimated coefficients.

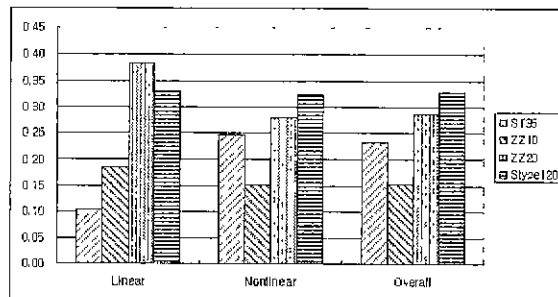


Figure 28. Comparison of estimation performance.

## References

1. Hwang, W.Y., 1980, Application of System Identification to Ship Maneuvering, PhD thesis, MIT
2. Kang, C.G., Seo, S.H., Kim, J.S., 1984, Maneuverability Analysis of a Ship by System Identification Technique, SNAK, Vol.21 No.4
3. Ahn, J.H., 1992, Estimation of Hydrodynamic Derivatives of a Ship Employing System Identification Method, M.S. Thesis, Seoul National University
4. Lee, K.C., Kim, J.K., Rhee K.P., 1995, Estimation of Hydrodynamic Derivatives by Parallel Processing of Second Order Filter, Journal of Hydrospace Technology, Vol.1, No.1, pp.66-74
5. Hwang, Y.S., 1996, An Estimation of Ship Maneuvering Equation by System Identification Method, M.S. Thesis, Seoul National University
6. Hirono, M., 1980, On Calculation Method of Ship Maneuvering Motion at Initial Design Phase, Journal of SNAJ, Vol.147 (Japanese)
7. Japan Institute of Navigation, 1995, Research on Ship Manoeuvrability and its Application to Ship Design, The 12th Marine Dynamic Symposium (Japanese), pp.91-133
8. Inoue, S., Hirono, M., Kijima, K., Takashima, J., 1981. A Practical Calculation Method of Ship Manoeuvring Motion, ISP, Vol.28, No.325
9. Japan Institute of Navigation, 1987, Research on Ship Manoeuvrability and its Application to Ship Design, The 4th Marine Dynamic Symposium (Japanese)
10. Korea Institute of Machinery and Materials(KIMM), 1988, Development of Maneuverability Prediction Technique, KIMM Report UDC 629.116
11. Son, K.H., 1989, On the Mathematical Model for Estimating the Manoeuvring Performance of Ships, Society of Korea Voyage, Vol.13, No.2
12. Lewis, F.L., 1986, Optimal Estimation - with an introduction to stochastic control theory, John Wiley & Sons, Inc.
13. Abkowitz, M.A., 1964, Lectures on Ship Hydrodynamics Steering and Maneuverability, Report No. Hy-5, Hydrodynamic Department Hydro-og Aerodynamisk Laboratorium, Lyngby, Denmark
14. Abkowitz, M.A., 1980, Measurement of Hydrodynamic Characteristics from Ship Maneuvering Trials by System Identification, SNAME Transaction Vol. 88
15. Abkowitz, M.A., 1988, Measurement of Ship Resistance, Powering and Maneuvering Coefficients from Simple Trials during a Regular Voyage, SNAME Transaction Vol.96
16. Crane, C.L., 1979, Maneuvering Trials of a 278,000-DWT Tanker in Shallow and Deep Waters, SNAME Transaction Vol. 87
17. Institute of Ship Engineering, Korea Maritime University, 1990, On the Analysis of Manoeuvrability of Start, Stop, Astern and Low speed
18. Lee, S.W.. 1997, Estimation of Maneuvering Coefficients form PMM Test by System Identification Method, M.S Thesis, Seoul National University
19. Rhee, K.P., 1981, Development and Education of the program to estimate the manoeuvrability of ship, Institute of Production Technology, Seoul National University
20. Ryu, M.C., 1992, Analysis of Planar Motion Mechanism Test by System Identification Method, M.S. Thesis, Seoul National Univeristy